High-Dimensional Solid-Liquid Phase Diagrams Involving Compounds and Polymorphs

Christianto Wibowo and Ketan D. Samant
Dept. of Chemical Engineering, University of Massachusetts, Amherst, MA 01003

Ka M. Ng
Dept. of Chemical Engineering, Hong Kong University of Science and Technology, Clear Water Bay, Hong Kong

A systematic procedure for the generation and visualization of high-dimensional isobaric phase diagrams for systems exhibiting compound formation and/or polymorphism is presented. Such phase diagrams are useful in synthesizing crystallization-based separation processes for systems involving compounds and polymorphs, which are common in the production of pharmaceuticals. Polythermal as well as isothermal phase diagrams of multicomponent systems can be generated. Examples are provided to illustrate the procedure.

Introduction

Crystallization-based separation processes are widely used in the production of solid commodity chemicals, fine chemicals, and pharmaceuticals (Tavare, 1995; Collet, 1999). Recently, systematic procedures for synthesizing these processes have been developed, with the aim of coming up with a reliable, optimal process while minimizing development time and effort (Cisternas and Rudd, 1993; Dye and Ng, 1995a,b; Berry and Ng, 1996, 1997; Berry et al., 1997; Wibowo and Ng, 2000; Schroer et al., 2001). All of these procedures rely on the visualization of the solid-liquid phase diagrams of the system under consideration.

Visualization of solid-liquid phase diagrams in two- and three-dimensional (2-D and 3-D) plots has been a routine practice for decades (Purdon and Slater, 1946; Ricci, 1966; Hasse and Schönert, 1969). However, many systems encountered in practice are multicomponent in nature, and cannot be completely represented by such plots. A procedure for generating and visualizing the multicomponent solid-liquid phase diagram for simple eutectic systems have been proposed (Samant et al., 2000). However, it is well known that the phase diagram of many real systems may involve features such as compound or adduct formation. In fact, adduct formation has been exploited in industrial crystallization-based separation processes, such as separation of *p*- and *m*-cresol (Tare and Chivate, 1976) and recovery of bisphenol-A from its mixture with phenol (Iimuro et al., 1990). Another complexity in the phase diagram can arise because of polymorphism. Crystallization of a substance in the right crystal form is very important, especially in the pharmaceutical industry, since most process patents only cover a specific polymorph of a drug. It is highly advantageous to be able to view high dimensional phase diagrams exhibiting these complex behaviors.

This article presents a systematic procedure for the generation and visualization of high-dimensional isobaric phase diagrams for systems exhibiting compound formation and/or polymorphism. In these systems, the components may combine to form different compounds, and each solute can crystallize in more than one form. The phase diagram of systems with compounds can be easily generated and visualized by treating them as reactive systems. Those with polymorphs are generated by identifying the stable modification under the given conditions. The only required input information is thermodynamic data such as activity coefficients, heats of fusion, and reaction equilibrium constants.

Isobaric Phase Behavior of Reactive Systems

Let us consider a c-component system with r reactions. The total number of variables in an isobaric system is c, that is, the mole fractions of $(c-1)$ components plus temperature. Therefore, the isobaric phase diagram is c-dimensional. By first ignoring the reactions, we can write phase equilibrium equations to identify *saturation varieties*. The definition of this term, along with other special terms for high-dimensional phase diagrams, is given in Table 1. Interested readers are referred to Wibowo and Ng (2002) for more detailed explanations. In general, a saturation variety of dimension m

Correspondence concerning this article should be addressed to K. M. Ng.
Current address for C. Wibowo and K. D. Samant: CWB Technology, 20311 Valley Blvd., Suite C, Walnut, CA 91789.

represents compositions at which $(c-m)$ components are co-saturated. The r reaction equilibrium equations involve nonlinear functions in mole fractions and temperature

$$\prod_{i=1}^{c} (\gamma_i x_i)^{\nu_{ij}} = K_j(T); \qquad j=1,2,\ldots,r \tag{1}$$

These equations can be geometrically interpreted as an object of dimension $(c-r)$ in the composition space. Since both phase and reaction equilibrium equations must be satisfied, the phase diagram of the reactive system is the intersection of this object with the saturation varieties. Consequently, saturation varieties of dimension $m<r$ will not survive the reactions. Saturation varieties of dimension $m \geq r$, if they survive the reactions, will appear as entities of dimension $(m-r)$.

As an illustration, consider a ternary system consisting of components A, B, and a compound C, formed through the reaction

$$A+B=C;\ K=\frac{(\gamma_c x_c)}{(\gamma_A x_A)(\gamma_B x_B)} \tag{2}$$

For simplicity, it is assumed that the reaction equilibrium constant does not depend on temperature. Figure 1 sketches the isobaric phase diagram for this system. The saturation varieties (in this case, saturation surfaces) for A, B, and C,

Table 1. Glossary of Special Terms for High-Dimensional Phase Diagrams

Adjacency matrix, $A=(a_{ij})$: A matrix whose row and column headings correspond to the vertices of digraph G; its elements are defined as

$$a_{ij}=\begin{cases}1 & \text{if } v_i \text{ is adjacent to } v_j\\ 0 & \text{else}\end{cases}$$

Adjacent vertices: Vertex v_i is adjacent to v_j if there is a directed edge from v_i to v_j.

Canonical coordinates: A set of coordinates used to plot aprojective subspace. It appears naturally once the projection rays have been defined.

Compartment: A subspace in a polythermal projection within which a component can be crystallized in pure form.

Cut: A picture obtained by viewing a part of the system and ignoring the rest. An m-dimensional cut of an n-dimensional object is an intersection between the object with a variety of dimension m.

Isoplethal cut: A cut of an isobaric phase diagram or its projection, taken at a constant composition of one or more component.

Isothermal cut: A cut of an isobaric temperature-composition phase diagram taken at a constant temperature.

Digraph, $G_l^k=(V_l^k, E_l^k)$: A discrete mathematical model representing the phase diagram of a system. It consists of a set of **vertices** V_l^k connected to each other by a set of **edges** E_l^k, and each edge $e_{ij}\in E_l{}^k$ has a direction from an initial vertex $v_j\in V_l^k$ to a terminal vertex $v_j\in V_l^k$. The superscript $k=M$, R, or I indicates molecular, reactive, or ionic system, respectively. The subscript $l=P$ or PT indicates isobaric or isobaric isothermal, respectively.

Eutectic: A eutectic of order n (**binary eutectic** if $n=2$, **ternary eutectic** if $n=3$, and so on) is a liquid mixture of n components, the composition of which is such that no other mixture of the same n components has a lower melting point.

Projection: An image obtained by shining light on an object. An m-dimensional projection of an n-dimensional object is the image of the object on an m-dimensional projective subspace (which can be a plane or any other geometrical feature). The line connecting the light source, a point in the object, and the image of the point in the projection is called a **projection ray**.

Central projection: A projection in which all projection rays pass through a point called the center of projection.

Jänecke projection: A central projection with a vertex representing a pure component in the system (usually the solvent) being the center of projection.

Parallel projection: A projection in which all projection rays are parallel.

Polythermal projection: A parallel projection along the temperature axis.

Reaction-invariant projection: A projection along stoichiometric varieties. In this projection, a reactive mixture of a given initial composition appears as a single point on the projective subspace, regardless of the extent of reaction.

Saturation variety matrix, $S=(s_{ij})$: A matrix whose row and column headings correspond to the saturation varieties and vertices of digraph G, respectively; its elements are defined as

$$s_{ij}=\begin{cases}1 & \text{if vertex } v_{ij} \text{ lies on saturation variety } i\\ 0 & \text{else}\end{cases}$$

Transformed mole fraction coordinates: A set of canonical coordinates for plotting the composition of reactive mixtures in a reaction-invariant projection. Often referred to as **transformed coordinates.**

Variety: A general term for an m-dimensional geometrical object in space. The variety is a **point** if $m=0$, a **curve** or **trough** if $m=1$, a **surface** if $m=2$, and a **volume** if $m=3$, or a **hypervolume** if $m>3$.

Saturation variety: A variety on the phase diagram, bounded by vertices and edges, inside which one or more components are saturated. A saturation variety of order n (**single saturation variety** if $n=1$, **double saturation variety** if $n=2$, and so on) has n saturated components.

Stoichiometric variety: A variety on the phase diagram describing composition changes due to reactions. The dimension of the stoichiometric variety is always the same as the number of independent reactions.

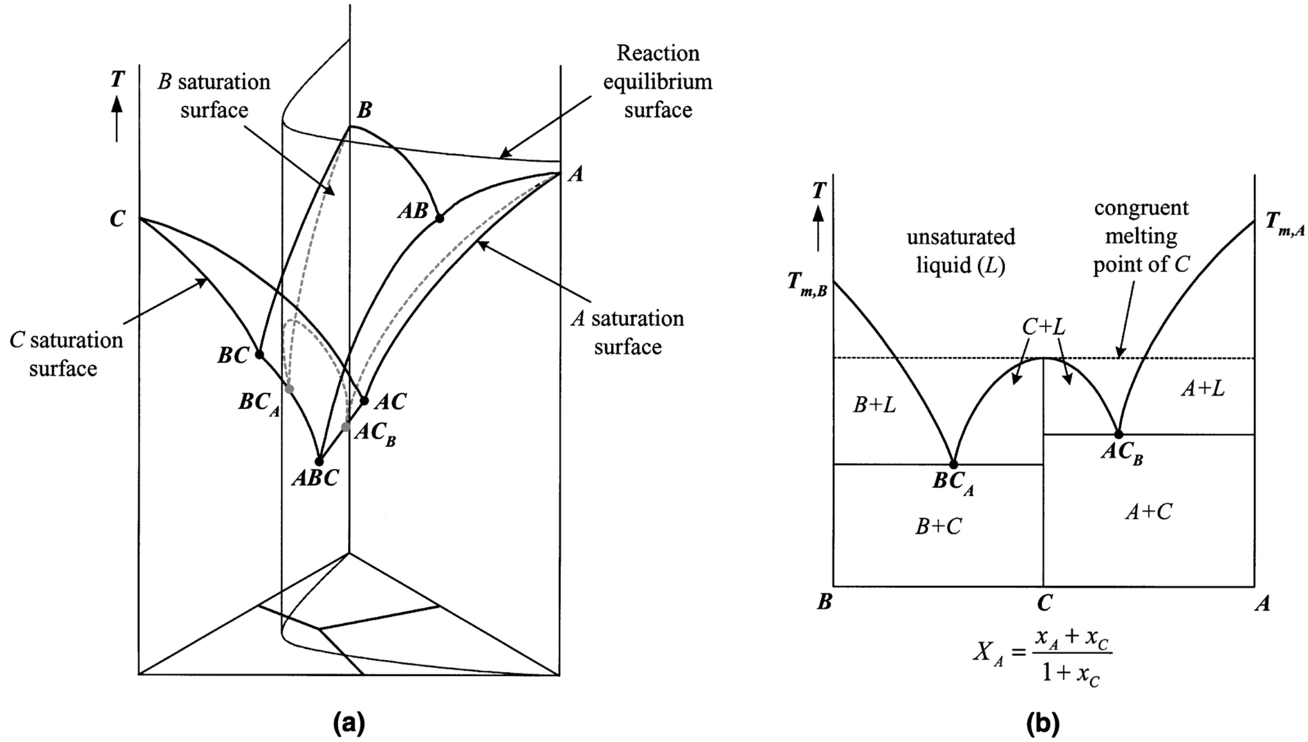

Figure 1. Isobaric phase diagram of a binary system with congruent melting compound.

(a) $T - x$ diagram with the compound considered as a third component; (b) binary $T - x$ diagram.

that is, *A-AB-ABC-AC*, *B-BC-ABC-AB*, and *C-AC-ABC-BC*, respectively, are indicated in the figure. The presence of reaction confines the possible compositions to the intersection of the saturation surfaces with the reaction equilibrium surface, indicated by the dashed curve in Figure 1a. The reaction-invariant projection of the composition space onto the *AB* face of the prism is depicted in Figure 1b, where compositions are plotted in transformed coordinates. It is clear that the binary eutectics *AB*, *AC*, and *BC*, as well as the ternary eutectic *ABC*, do not survive the reaction, because their compositions do not satisfy the reaction equilibrium equation. Because the reaction equilibrium surface does not intersect the AB double saturation trough, there is no region corresponding to $A + B$ co-saturation in Figure 1b. However, it intersects the *AC* and *BC* double saturation troughs, giving rise to two vertices: AC_B and BC_A. Note that these vertices can be referred to as reactive eutectics, since their appearance is caused by the reactions. They are labeled after the saturated components, while unsaturated components are indicated as subscripts.

The system depicted in Figure 1 exhibits *congruent melting* behavior. The parabolic curve between BC_A and AC_B (see Figure 1b), which is a part of the original *C* saturation surface, has a maximum at the composition of the compound ($X_A = X_B = 0.5$). At this maximum point, compound *C* exists in stable equilibrium with a solution of the same composition. The temperature at this point is called the congruent melting point of *C*, which is different from the melting point of solid *C*. A similar system with a different reaction equilibrium constant is depicted in Figure 2. Notice that the reaction-invariant projection of the phase diagram shows a monotonic curve connecting BC_A and AC_B (Figure 2b). Above the temperature of AC_B, solid *C* cannot exist and appears to decompose to give a solution saturated with *A*. Such a system is said to exhibit *incongruent melting* behavior, and the transition temperature is called the incongruent melting point of *C*. AC_B can be referred to as a reactive peritectic.

Different polymorphs of a substance have different melting points and heats of fusion, but they are indistinguishable in liquid form. At a given temperature, only the modification with the lowest solubility is stable. Therefore, the solid-liquid phase diagram involving a component that can crystallize in several forms shows regions corresponding to different polymorphs. For example, consider a binary system of component *A*, which can crystallize in two different modifications (A^α and A^β), and a solvent *B*. Above a transition temperature, only the β-modification can coexist with a solution saturated with *A*. On the other hand, only the α-modification is stable below the transition temperature. The transition temperature between different forms, often referred to as the *crossover temperature*, is independent of the solvent (Beckmann, 2000).

The binary phase diagram for the above binary system can be generated by calculating the saturation curves of both polymorphs (Figure 3). The saturation curve of *A* is made up of parts of the two saturation curves of the polymorphs, as indicated by the solid curve. At each temperature, the point corresponding to the lowest mole fraction of *A* is taken. The other parts of the saturation curves form the dotted curve, which corresponds to metastable conditions. The transition point between the two polymorphs is labeled as $A_B^{\alpha\beta}$, signifying the saturation of both A^α and A^β, while *B* is unsaturated.

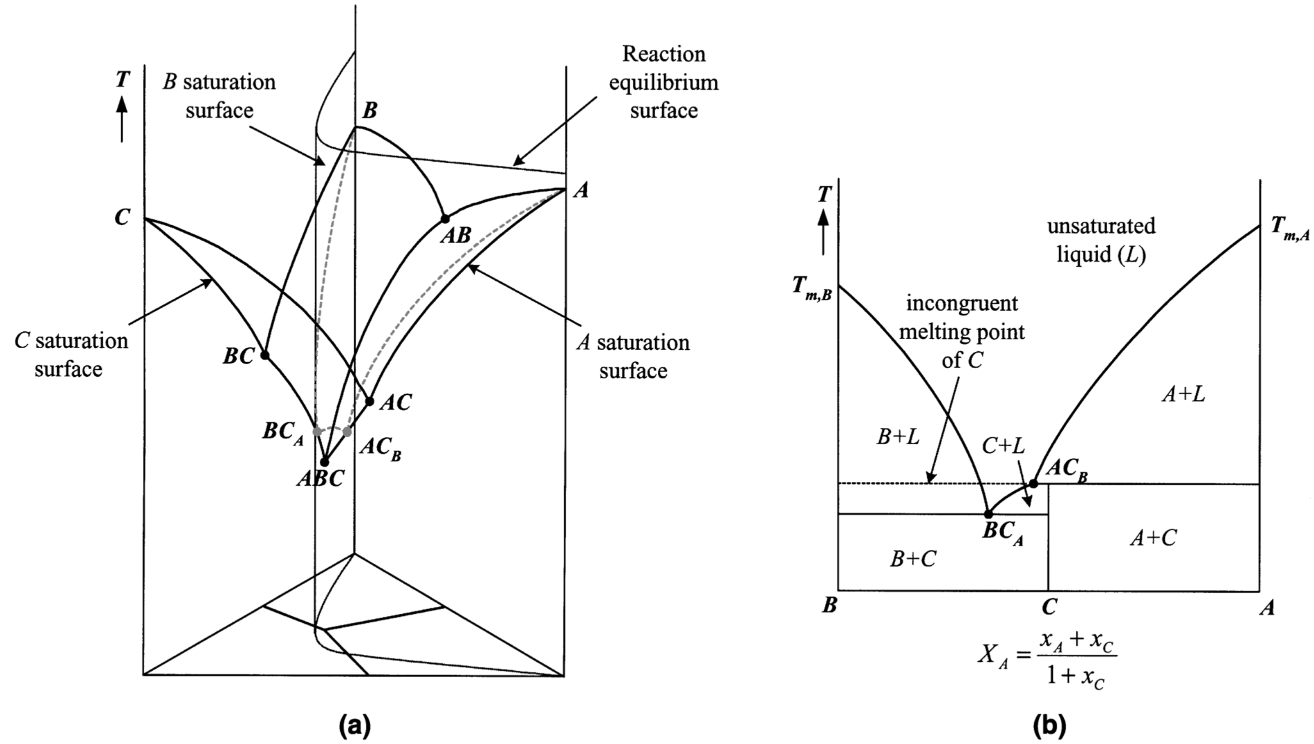

Figure 2. Isobaric phase diagram of a binary system with incongruent melting compound.

(a) $T - x$ diagram with the compound considered as a third component; (b) binary $T - x$ diagram.

Generation and Visualization of Isobaric Reactive Phase Diagrams

Following Samant et al. (2000), an isobaric reactive phase diagram can be represented as a digraph $G_P^R = (V_P^R, E_P^R)$. Saturation varieties are defined by the vertices $\in V_P^R$, which are connected by edges $\in E_P^R$ according to an adjacency matrix. The phase diagram can be generated by identifying and locating all vertices and edges in the digraph. Obviously, all reactions, as well as the expressions for reaction equilibrium constants, must be specified.

Identification and location of vertices $\in V_P^R$

The vertices in an isobaric reactive phase diagram include vertices which survive the reactions, referred to as *nonreactive vertices*, as well as new vertices generated by the reactions, referred to as *reactive vertices*. A simple and efficient algorithm for identifying and locating the vertices is listed in Table 2. The algorithm searches for surviving nonreactive vertices first. If a vertex does not survive the reactions, then reactive vertices with the same saturated components are sought. Note that there can be more than one vertex having the same saturated components. The search begins with vertices containing two saturated components, and proceed until reaching vertices containing $(c - r)$ saturated components. All solutions are checked for consistency. Although the algorithm appears to be very time consuming, as $c - r \leq 3$ for most reactive systems, the search for vertices actually ends quickly even for large values of c.

In the search for reactive vertices, it is useful to know that a vertex contains only a limited number of unsaturated components. The following theorem applies:

Theorem 1. *The number of unsaturated components in a reactive vertex $\in V_P^R$ saturated with n components $(2 \leq n \leq c - r)$ varies from 1 to r.*

Proof. In an isobaric c-component system with n saturated components and r reactions, there are $(n+1)$ phases in equilibrium (n solid phases and one solution). Therefore, according to Gibbs phase rule, the number of degrees of freedom is $f = c - (n+1) - r + 1 = c - n - r$. Because $f = 0$ for a vertex, we deduce that $c - n = r$. The number of unsaturated components in the system can be obtained by simply subtracting the number of saturated components from the total number of components. The result is $c - n$, which is also equal to r. However, depending on the reaction scheme, it is possible that some of the r reactions do not have an effect on the vertex in question. In such a case, the number of unsaturated components would be less than r.

To illustrate this point, consider a system containing a total of five components and two reactions $(r = 2)$

$$A = B; \quad K_1 = \frac{\gamma_B x_B}{\gamma_A x_A} \tag{3a}$$

$$C + D = E; \quad K_2 = \frac{(\gamma_E x_E)}{(\gamma_C x_c)(\gamma_D x_D)} \tag{3b}$$

Let us focus on a reactive vertex saturated with B and C $(n = 2)$, assuming it exists. From phase equilibrium equations, the values of x_B and x_C can be obtained. Equation 3a allows the determination of x_A, but Eq. 3b does not give a unique solution for x_D and x_E. This means vertex BC_{ADE} can never be present. If we now set $x_D = x_E = 0$ and ignore Eq. 3b, a

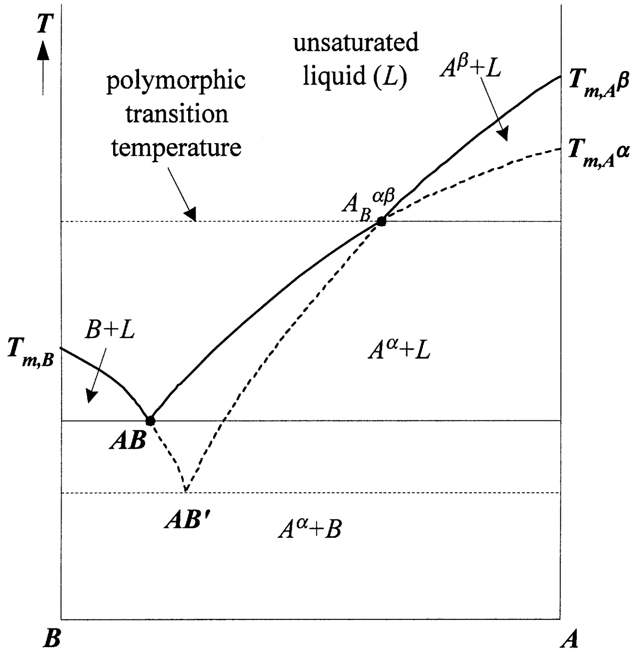

Figure 3. Isobaric phase diagram of a binary system exhibiting polymorphism.

unique solution can be obtained. This indicates the presence of vertex BC_A, which only contains one unsaturated component. It can be said that this vertex survives the second reaction, or, the second reaction does not have any effect on this reactive vertex created by the first reaction.

The situation is different for another system, which involves the same five components but a different set of reactions

$$A + B = C; \quad K_1 = \frac{(\gamma_C x_C)}{(\gamma_A x_A)(\gamma_B x_B)} \tag{4a}$$

$$A + C = E; \quad K_2 = \frac{(\gamma_E x_E)}{(\gamma_A x_A)(\gamma_C x_C)} \tag{4b}$$

D is not involved in the reactions. Again, consider a reactive vertex saturated with B and C. For this system, Eqs. 4a and 4b allow the determination of both x_A and x_E. In other words, reactive vertex BC_{AE}, which contains two unsaturated components, is present.

If polymorphs are involved, the calculation must take into account the solubilities of the different modifications. In other words, if component i can crystallize in several polymorphic forms, then

$$x_i^{\text{sat}} = \frac{1}{\gamma_i} \min_j \left\{ \exp\left[\frac{\Delta H_{m,i^j}}{R} \left(\frac{1}{T_{m,i^j}} - \frac{1}{T} \right) \right] \right\} \tag{5}$$

where j indicates the different modifications. There are also additional vertices corresponding to polymorphic transition points. However, it is more convenient to identify these vertices while calculating the edges. At this point, only the transition temperatures between modifications need to be calculated. Table 3 shows a simple algorithm for calculating these transition temperatures from the heat of fusion and melting point data.

Table 2. Algorithm for Calculation of Vertices $\in V_P^R$ Using a Thermodynamic Model

- At any vertex $\in V_P^R$, there are n components saturated at equilibrium. Let these components be denoted by indices 1 to n.
- There are also p saturated components ($0 \leq p \leq r$). Let these components be denoted by indices $(n+1)$ to $(n+p)$.
- The other $(c-n-p)$ components are not present. Thus, $x_i = 0$ for $i = n+p+1, \ldots, c$.
- Thus, there are $n+p+1$ variables ($x_1, \ldots, x_{n+p}$, and T), which must be determined by solving a set of $n+p+1$ equations (n phase equilibrium equations, p reaction equilibrium equations, and 1 mole fraction balance equation).

Search Procedure

A1. Pick n saturated components.

A2. Let $p = 0$ (in other words, set $x_i = 0$ for $i = n+1, \ldots, c$).

A3. Check each of the r reaction equilibrium equations. Remove the equation if

$$\prod_{i=1}^{c} (\gamma_i x_i)^{\nu_{ij}} = \frac{0}{0}$$

If no reaction equilibrium equation remains, then a nonreactive vertex is found. Proceed to the calculation procedure to solve the set of $(n+1)$ equations. Otherwise, increase p by one.

A4. Choose p components among the remaining $(c-n)$ components, and set their concentrations to be nonzero. Repeat the check in step A3. If no reaction equilibrium equation remains, then a reactive vertex is found. Proceed to the calculation procedure to solve the set of $(n+p+1)$ equations. Otherwise, increase p by one and repeat, or stop if $p = r$.

A5. Repeat step A4 using different choices for the p components. Each time a reactive vertex is found, proceed to the calculation procedure. Stop when all combinations have been considered.

Calculation Procedure

B1. Initalize γ_i, $i = 1$, $n+p$ to unity.

B2. Pick an initial guess for T. At this T, pick $x_i = x_i^{\text{sat}}$, $i = 1, \ldots, n$ and $x_i < x_i^{\text{sat}}$, $i = n+1, \ldots, n+p-1$ as initial guesses. Calculate the last mole fraction as

$$x_{n+p} = 1 - \sum_{i=1}^{n+p-1} x_i$$

B3. Calculate γ_i, $i = 1, \ldots, n+p$ using a thermodynamically consistent model.

B4. Calculate the following $n+p$ functions

$$F_j = \begin{cases} \dfrac{1}{\gamma_j} \exp\left[\dfrac{\Delta H_{m,j}}{R} \left(\dfrac{1}{T_{m,j}} - \dfrac{1}{T} \right) \right] - x_j^{\text{sat}} & j = 1, \ldots, n \\ \displaystyle\prod_{i=1}^{c} (\gamma_i x_i)^{\nu_{i,j-n}} - K_{j-n}(T) & j = n+1, \ldots, n+p \end{cases}$$

B5. If $|\boldsymbol{F}| > \boldsymbol{\epsilon}$ (a vector of set tolerances), then go to step B2 and simultaneously update the values of the guesses, using Newton's method with a finite different approximation to the Jacobian. Otherwise stop.

B6. Check the solution for consistency. In other words, ensure that $x_i = x_i^{\text{sat}}$, $i = 1, \ldots, n$, $x_i < x_i^{\text{sat}}$, $i = n+1, \ldots, n+p$, and $0 \leq x_i \leq 1$ $\forall i$. Record all consistent solutions.

Identification and calculation of edges $\in E_P^R$

After identifying all vertices, we then identify the edges $\in E_P^R$, which connect adjacent vertices. This is done using

Table 3. Algorithm for Identifying and Calculating Polymorphic Transition Temperature

(1) Pick two modifications, j and k, where $T_{m,j} > T_{m,k}$.

(2) Solve

$$\Delta H_{m,j}\left(\frac{1}{T_{m,j}} - \frac{1}{T}\right) = \Delta H_{m,k}\left(\frac{1}{T_{m,k}} - \frac{1}{T}\right)$$

(3) If $T > T_{m,j}$, the transition temperature between modification j and k does not exist.
If $T < T_{m,j}$, calculate

$$f_i = \exp\left[\frac{\Delta H_{m,i}}{R}\left(\frac{1}{T_{m,i}} - \frac{1}{T}\right)\right]$$

for all modifications, and go to Step 4.

(4) Determine if modification j has the lowest solubility. In other words, check if

$$f_j = \min_i f_i$$

If so, then T is the transition temperature between modification j and k. Otherwise, the transition temperature does not exist.

(5) Repeat Steps 2 to 4 for all possible combinations of j and k, where $T_{m,j} > T_{m,k}$.

three adjacency rules, summarized in Table 4. The results can be displayed in the form of an adjacency matrix. Due to the non-linearity of reaction equilibrium equations, it is inaccurate to connect the vertices with straight lines. Therefore, the edges should be computed using the algorithm presented in Table 5.

If one or more components saturated on an edge can crystallize as different polymorphs, and the edge spans over a temperature range which includes any of the transition temperatures, then the edge must be subdivided by adding vertices corresponding to polymorphic transition points. These new vertices can be calculated using the algorithm of Table 5, with T fixed at the transition temperature in Step C3. The adjacency matrix must then be modified to reflect this subdivision. In addition, the connections between the new vertices must be added to the adjacency matrix. These can be determined using adjacency rules 1 and 2, with the additional requirement that the same modifications are saturated at both v_i and v_j.

Table 4. Adjacency Rules (Samant et al., 2000)

Rule 1. v_i is adjacent to v_j if:

- v_j has more components than v_i and has all components in v_i,
- all the components saturated at v_i is also saturated at v_j,
- v_j has one additional saturated component.

Rule 2. v_i is adjacent to v_j if:

- v_i and v_j have the same number of saturated components,
- all the components saturated at v_i are also saturated at v_j.

Rule 3. v_i is adjacent to v_j if:

- v_i and v_j have the same components and the same number of saturated components,
- all but one components saturated at v_i are also saturated at v_j.

Table 5. Algorithm for Calculation of Edges $\in E_P^R$ Using a Thermodynamic Model

- Along any edge $\in E_P^R$, there are n components saturated at equilibrium. These are the components saturated at *both* $v_i \in V_P^R$ and $v_j \in V_P^R$ (the vertices connected by the edge). Let these components be denoted by indices 1 to n.
- If there is a component that is saturated in v_j, but not in v_i, let this component be denoted by $(n+1)$. Otherwise, let a component that is present in v_j, but not in v_i be denoted by $(n+1)$.
- There are also p other components $(0 \le p \le r)$, which are unsaturated in both v_i and v_j. Let these components be denoted by indices $(n+2)$ to $(n+p+1)$.
- Thus, there are $n+p+2$ variables $(x_1, \ldots, x_{n+p+1}$, and $T)$, which must be determined by solving a set of $n+p+1$ equations (n phase equilibrium equations, p reaction equilibrium equations, and 1 mole fraction balance equation).

Calculation procedure

C1. Initialize γ_i, $i = 1, \ldots, n+p+1$ to unity.

C2. Vary x_{n+1} between 0 and x_{n+1}^{sat}, starting from x_{n+1}^{sat}. Follow steps C3 to C7 for each value of x_{n+1} to obtain the edge. Stop when the other vertex is reached.

C3. Pick an initial guess for T. At this T, pick $x_i = x_i^{\text{sat}}$, $i = 1, \ldots, n$ and $x_i < x_i^{\text{sat}}$, $i = n+2, \ldots, n+p$ as initial guesses. Calculate the last mole fraction as

$$x_{n+p+1} = 1 - \sum_{i=1}^{n+p} x_i$$

C4. Calculate γ_i, $i = 1, \ldots, n+p+1$ using a thermodynamically consistent model.

C5. Calculate the following $n+p$ functions

$$F_j = \begin{cases} \dfrac{1}{\gamma_j}\exp\left[\dfrac{\Delta H_{m,j}}{R}\left(\dfrac{1}{T_{m,j}} - \dfrac{1}{T}\right)\right] - x_j^{\text{sat}} & j = 1, \ldots, n \\ \displaystyle\prod_{i=1}^{c} (\gamma_i x_i)^{v_{i,j-n}} - K_{j-n}(T) & j = n+1, \ldots, n+p \end{cases}$$

C6. If $|\boldsymbol{F}| > \boldsymbol{\epsilon}$ (a vector of set tolerances), then go to step C3 and simultaneously update the values of the guesses, using Newton's method with a finite difference approximation to the Jacobian. Otherwise stop.

C7. Record all consistent solutions.

Once all the vertices and edges have been determined, we can identify the saturation varieties. This can be done by reading across the rows of the saturation variety matrix $\boldsymbol{S}$, which can be generated from the adjacency matrix $\boldsymbol{A}$

$$\boldsymbol{S} = \text{boolean}\left[(\boldsymbol{A} + \boldsymbol{I})^{c_{\max} - c_{\min}}\right] \tag{6}$$

where $c_{\max}$ and $c_{\min}$, respectively, are the maximum and minimum number of saturated components at the vertices of the digraph. The boolean operator turns all elements greater than unity to unity.

To plot the reactive phase diagram thus generated, the transformed mole fraction coordinates are used. Since the transformed mole fractions reduce the dimensionality of the system using the r reaction equilibrium equations, there are $(c-r)$ independent coordinates. The reactive phase diagram can be plotted on the plane of the paper as is for $c-r=2$, or as a polythermal projection for $c-r=3$. For $c-r>3$, we use multiple projections of the polythermal projection. As far as process synthesis is concerned, polythermal projections are most useful (Wibowo and Ng, 2000). However, it is also desirable to generate isothermal cuts, which will be discussed next.

Generation and Visualization of Isobaric Isothermal Reactive Phase Diagrams

An isobaric isothermal reactive phase diagram, represented as $G^R_{PT} = (V^R_{PT}, E^R_{PT})$, is an isothermal cut of G^R_P. Since temperature is fixed, the isothermal cut of a c-component system with r reactions is $(c-r-1)$-dimensional. Therefore, only saturation varieties with $(c-r-1)$ or less saturated components can appear in the cut.

A vertex $\in V^R_{PT}$ is the intersection of an edge $\in E^R_P$ with the variety of constant temperature (a line if $c-r=2$, a plane if $c-r=3$, or a hyperplane if $c-r>3$). Therefore, the vertices $\in V^R_{PT}$ can be identified by solving the functional relationship representing the edges $\in E^R_P$ at the specified temperature. In contrast to molecular systems without reactions, the identification of vertices $\in V^R_{PT}$ and edges $\in E^R_{PT}$ is not as straightforward. This is due to the nonmonotonic nature of the edges $\in E^R_P$. The two major complications that arise are:

(a) There can be multiple solutions from such an intersection, resulting in two or more vertices, $\in V^R_{PT}$, to be referred to as *constituent vertices*, that belong to the same edge $\in E^R_{PT}$;

(b) There can be saturation varieties that do not have any vertex $\in V^R_{PT}$ or any edge $\in E^R_{PT}$. These complications can be overcome by using the information from the molecular phase diagram without reaction G^M_P, as discussed below.

Identification and location of vertices $\in V^R_{PT}$

For each edge $\in E^R_P$, we use an algorithm similar to Table 5 to determine vertices $\in V^R_{PT}$, if any, that lie on the edge. The only difference in the calculation procedure is that instead of varying x_{n+1} in step C2, we fix T. The following theorem is useful in the identification process:

Theorem 2. *The number of unsaturated components in a reactive vertex $\in V^R_{PT}$ saturated with n components ($2 \leq n \leq c-r-1$) can vary from 1 to $(r+1)$.*

The proof is similar to the one for Theorem 1. Vertices in G^R_{PT} are labeled according to the saturated and unsaturated components along the edge.

Identification and calculation of edges $\in E^R_{PT}$

Once all vertices $\in V^R_{PT}$ have been identified, the adjacency matrix can be developed using the rules in Table 4. While applying these rules, two or more constituent vertices $\in V^R_{PT}$ belonging to the same edge $\in E^R_P$ are at first considered as one vertex, referred to as a *multiple vertex.* This vertex is then decomposed to form the constituent vertices, which have exactly the same saturated and unsaturated components at different compositions. These constituent vertices are distinguished from each other by Roman numeral superscripts. The adjacency matrix is then refined. In this refinement process, we need to take into account the limitations on the number of edges that start or end at a vertex. We have the following theorem:

Theorem 3. *There can only be one edge connecting a vertex $\upsilon_i \in V^R_{PT}$ containing n saturated components to another vertex υ_j, which is saturated in all but one component saturated in υ_i.*

Proof. An edge connecting two vertices υ_i and υ_j is generated by changing the concentration of the component that is saturated in υ_i, but not in υ_j. Since there is only one variable to modify, there is only one degree of freedom, corresponding to only one edge.

Calculation results often indicate that when multiple vertices are involved, there can be more than one vertex υ_j that is saturated in all but one component saturated in $\upsilon_i \in V^R_{PT}$ with n saturated components. Strict adherence to Rules 1 to 3 in such a case would lead to a violation of Theorem 3. Therefore, an additional adjacency rule is needed for G^R_{PT}:

Rule 4. If a multiple vertex υ_i is adjacent to more than one vertex containing the same $(n-1)$ saturated components, then each constituent vertex is adjacent to only one such vertex. The exact correspondence can be determined by calculating the edges.

Any edge connecting a pair of vertices which turn out to be nonadjacent must be eliminated.

The total number of edges that start or end at a particular vertex q can be predetermined. The value of q depends on the number of saturated components in the vertex.

Theorem 4. *In a system with c components and r reactions, a vertex with one saturated component has a total of $q = c - r - 2$ edges*.

Proof. If only one component is saturated at a vertex, then there are two phases in equilibrium. Since the degree of freedom of a vertex is zero, the Gibbs phase rule implies that $c' - r' = 2$, where c' is the total number of components present at the vertex and r' is the number of reactions among these components. Clearly, the vertex lies on a variety representing a subset of the original system involving the c' components and r' reactions. Because the minimum number of phases is always one, and $c' - r' = 2$ for this subset, this variety is 1-D. Since the reactive vertex contains only one saturated component, the only way of creating an edge which starts at this vertex is by adding a component that is not present in the vertex. Such an edge would extend to the additional dimension created by the addition of the extra component. Note that this extra component provides only one additional degree of freedom, which implies that there can be only one edge for each additional dimension. Since the isobaric isothermal phase diagram of the system has a dimension of $(c-r-1)$, the reactive vertex in question can have $(c-r-2)$ edges.

Theorem 5. *In the system with c components and r reactions, a vertex $\in V^R_{PT}$ with n saturated components ($n \geq 2$) has a total of $q = c - r - 1$ edges.*

Proof. Because there are n saturated components, there must be $(n+1)$ phases in equilibrium. Using an argument similar to the one for proving Theorem 4, it can be shown that this vertex is a part of an n-dimensional variety of the phase diagram. A total of n edges can lie within this variety, each of which corresponds to a change in the concentration of one of the saturated components. There are also $(c-r-n-1)$ other edges emanating out of the n-dimensional variety, each of which corresponds to an increasing concentration of a component that is not present in the vertex. Hence, the total number of edges is $(c-r-1)$.

Corollary. *Because a vertex must have q edges, if any vertex υ_i is adjacent to k other vertices ($k > q$), then edges $(k-q)$ must be removed.*

We can also deduce that:

Rule 5. If after eliminating the excessive edges, each constituent vertex $\upsilon_i \in V^R_{PT}$ is adjacent to k other vertices ($k < q$), then the constituent vertices are connected to each other by $(q-k)$ different edges.

To calculate the edges $\in E^R_{PT}$, the algorithm in Table 5 can again be used. The only differences are that the number of unsaturated components is now $(p+1)$ and temperature is no longer a variable.

The saturation varieties can be identified by generating the saturation variety matrix using Eq. 6. However, in addition to these saturation varieties, there may exist other saturation varieties that do not have any vertex $\in V^R_{PT}$, and, thus, cannot be identified from the saturation variety matrix. Such a saturation variety must be at least 1-D, since otherwise it would appear as a vertex and appears in the saturation variety matrix. Accordingly, the saturation variety must have $(c-r-2)$ or less saturated components. A saturation variety without vertices can be present in G^R_{PT} if

$$\frac{T\left(v_i \in V^R_P\right)-T}{T\left(v \in V^M_P\right)-T} < 0 \quad \forall i \tag{7}$$

$T(v_i \in V^R_P)$ is the temperature at vertex v_i which bounds the same saturation variety in G^R_P, T is the specified temperature, and $T(v \in V^M_P)$ is the temperature at vertex v in G^M_P, which has exactly the same saturated components as the saturation variety in question. In other words, Eq. 7 states that the saturation variety can be present if T is above $T(v_i \in V^R_P)$, but below $T(v \in V^M_P)$, or vice versa. Such a saturation variety, if present, should be calculated using the procedure in Table 5, by appropriately selecting the saturated and unsaturated components.

Examples

To illustrate the ideas described above, let us now consider six examples. All systems are assumed to be ideal, and the required thermodynamic information such as heats of fusion, melting points, and reaction equilibrium constants, are available.

Example 1: ternary system with compound formation

Let us consider a ternary system comprising of A, B, and D with compound formation between A and B, described by the reaction

$$A+B=C; \quad K=\frac{(\gamma_C x_C)}{(\gamma_A x_A)(\gamma_B x_B)} \tag{8}$$

Table 6. Data for Ternary System with Compound Formation (Example 1)

Pure Component Data		
Compound	ΔH_m (J/mol)	T_m (K)
A	11,290	314.1
B	15,400	395.4
C	21,000	421.1
D	6,008	273.2
Reaction equilibrium constant: $K=\exp[E_1+(E_2/T)]$		
Reaction	E_1	E_2 (K)
$A+B=C$	-17.5	5,500

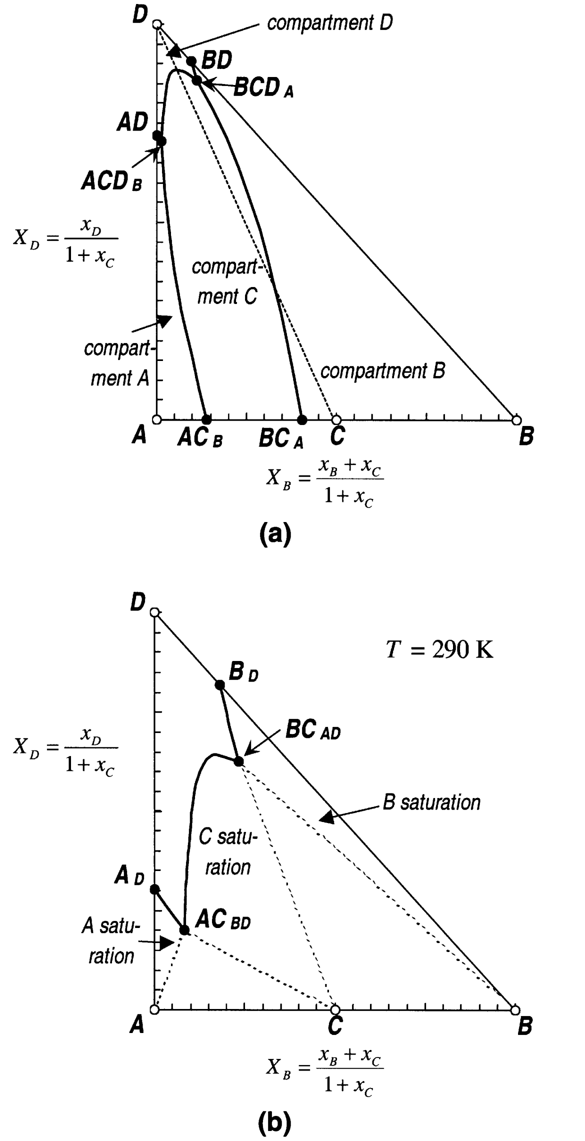

Figure 4. Isobaric phase diagram for ternary system compound formation (Example 1).

(a) Polythermal diagram; (b) isothermal cut at 390 K.

The thermodynamic parameters used for this system are listed in Table 6. Calculation results show that the system $A+B=C$ exhibits incongruent melting behavior, with an incongruent melting point at 317.7 K.

Figure 4a shows the polythermal projection of the reactive phase diagram, plotted in transformed coordinates. The vertices that survive the reaction include A, B, D, AD, BD (nonreactive vertices), AC_B, BC_A, ACD_B, and BCD_A (reactive vertices). The crystallization compartments are also indicated in the figure. It is interesting to note that due to the incongruent melting behavior, compartment C does not include the composition of the compound C itself. If a solution containing 50% A and 50% B is cooled below its saturation temperature, B will crystallize out instead of C. However, the situation changes as D is added into the mixture. As the dotted line CD indicates, if the equimolar mixture of A and

Table 7. **Data for Ternary System with Polymorphism (Example 2)**

Pure Component Data		
Component	ΔH_m (J/mol)	T_m (T)
$A(\alpha)$	23,600	375
$A(\beta)$	18,800	392
$A(\gamma)$	15,200	405
$A(\delta)$	11,250	415
B	17,500	400
D	12,100	353

B contains more than 40% D, then C will crystallize out first upon cooling.

Figure 4b is an isothermal cut of the reactive phase diagram at 290 K. The figure shows two vertices representing single saturation varieties (A_D and B_D) and two vertices representing double saturation varieties (AC_{BD} and BC_{AD}). The regions where each component is saturated are also indicated in the figure. The triangle A-C-AC_{BD} is the region where solids A and C are in equilibrium with a solution represented by AC_{BD}. Similarly, B-C-BC_{AD} is the region where solids B and C are in equilibrium with a solution represented by BC_{AD}.

Example 2: ternary system exhibiting polymorphism

Consider a system consisting of two solutes A and B, and one solvent D, where A can crystallize in four different polymorphic forms. The thermodynamic data for the different modifications, as well as for the other components, are given in Table 7. The crossover temperatures between modifications δ and γ, γ and β, and β and α are found using the algorithm of Table 3 to be 379 K, 345 K, and 321 K, respectively.

The polythermal diagram of the system is shown in Figure 5a. Because the temperature range between vertices A (415 K) and AD (324 K) includes $\gamma\delta$ and $\beta\gamma$ transition temperatures, the edge connecting these vertices is subdivided by adding two new vertices $A_D^{\gamma\delta}$ and $A_D^{\beta\gamma}$. Similarly, new vertices are added on edges AB-ABD and AD-ABD to reflect polymorphic transitions. There are four different compartments for A, one for each modification. Figure 5b shows two isothermal cuts. At 380 K, only modification δ is found, while at 330 K only modification β appears in the cut.

Example 3: ternary system exhibiting compound formation and polymorphism

This example illustrates a case where both compound formation and polymorphism occur. Consider a system of two solutes (A and B) and a solvent (D), where A and B can crystallize in 4 and 2 different polymorphic forms, respectively. There is also a 1:1 compound (C) formed between A and B. The input information is summarized in Table 8. Figure 6 shows the polythermal projection of the reactive phase diagram, indicating separate compartments for each modification of A and B. The transitions between modifications of A occur at 397 K, 355 K, and 307 K, while the transition from B^α to B^β occurs at 433 K. The phase behavior of this system is similar to that of the ternary system $AgNO_3-NH_4NO_3-H_2O$ reported in Ricci (1966).

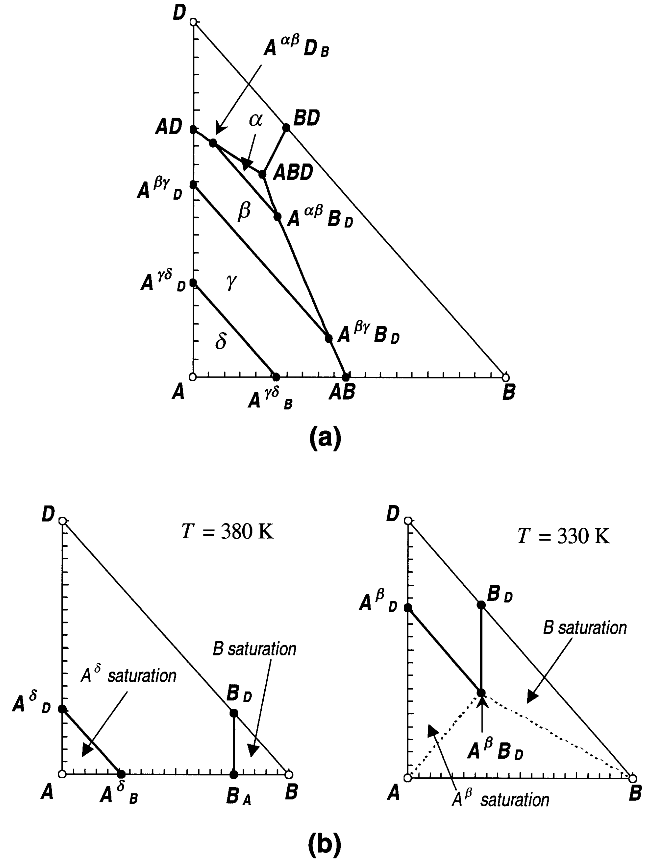

Figure 5. Isobaric phase diagram for ternary system with polymorphism (Example 2).

(a) Polythermal diagram; (b) isothermal cuts.

Example 4: ternary system with a ternary compound

This example illustrates the presence of a saturation variety without vertices. Consider an ideal system with a reaction forming a ternary compound

$$A + B + C = D; \quad K = \frac{(\gamma_D x_D)}{(\gamma_A x_A)(\gamma_B x_B)(\gamma_C x_C)} \tag{9}$$

Table 8. **Data for Ternary System with Both Compound Formation and Polymorphism (Example 3)**

Pure Component Data		
Component	ΔH_m (J/mol)	T_m (K)
$A(\beta)$	16,100	417
$A(\gamma)$	15,300	425
$A(\delta)$	13,700	435
$A(\epsilon)$	11,500	443
$B(\alpha)$	13,200	475
$B(\beta)$	11,500	482
C	18,000	443
D	6,000	273
Reaction equilibrium constant: $K = \exp[E_1 + (E_2/T)]$		
Reaction	E_1	E_2 (K)
$A + B = C$	-3.0	1,500

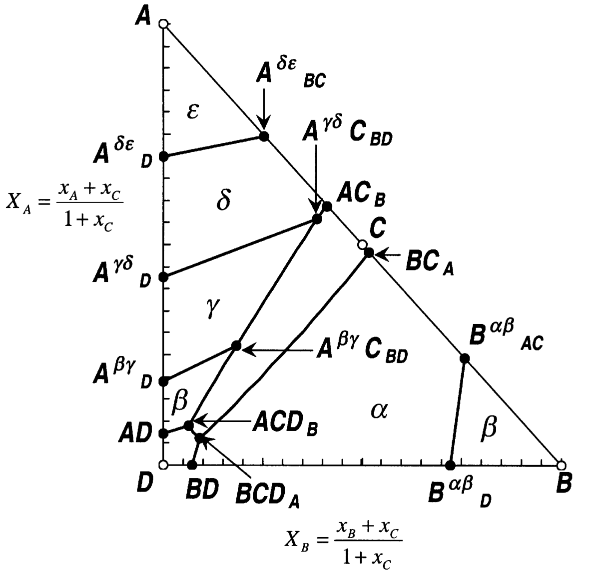

Figure 6. Isobaric phase diagram for ternary system with both compound formation and polymorphism (Example 3).

The thermodynamic data is summarized in Table 9. The polythermal projection of the phase diagram (Figure 7a) shows four compartments. Compartment D is bounded by the edges connecting vertices ABD_C, ACD_B, and BCD_A, all of which are reactive vertices. The temperatures corresponding to these vertices are 271.22 K, 272.84 K, and 274.98 K, respectively.

Let us generate two isothermal cuts at 285 K and 282 K, respectively. At 285 K, none of the edges connecting the reactive vertices appear in the cut (Figure 7b). The only vertices are A_B, A_C (corresponding to A saturation variety), B_A, B_C (corresponding to B saturation variety), C_A, and C_B (corresponding to C saturation variety). However, D saturation variety may also exist, as it satisfies Eq. 7. Calculations reveal this saturation variety, as shown in Figure 7b, which is an isola formed by the D-saturation curve.

Table 9. Data for Ternary System with a Ternary Compound (Example 4)

Pure Component Data		
Component	ΔH_m (J/mol)	T_m (K)
A	18,000	300
B	16,000	310
C	15,000	320
D	19,000	450
Reaction equilibrium constant: $K = \exp[E_1 + (E_2/T)]$		
Reaction	E_1	E_2 (K)
$A + B + C = D$	−2.4	850

At 282 K, an additional vertex (CD_{AB}) is identified (Figure 7c). This vertex has two constituent vertices, as indicated by the Roman numeral superscripts. Application of Rule 1 results in an edge connecting C_A to CD_{AB}, as well as another one connecting C_B to CD_{AB}. From each constituent vertex of CD_{AB}, there can only be one edge connecting it to a vertex saturated with C (Rule 4). Therefore, C_A is adjacent to one constituent vertex and C_B is adjacent to the other. In addition, since $c - r = 3$ for this system, there can only be one edge emanating from C_A and C_B (Theorem 4). Therefore, the edge connecting C_A and C_B must be removed. It can be clearly seen in the figure that this edge is actually interrupted by the D-saturation variety, such that it breaks up to form two new edges (C_A-CD^{I}_{AB} and C_B-CD^{II}_{AB}). Since each constituent vertex of CD_{AB} is only adjacent to one other vertex, they must be connected to each other by one edge (Rule 5). This edge defines the D saturation variety. It is interesting to note that the presence of multiple constituent vertices also divides the C saturation variety into two regions, indicated by the hatched triangles in Figure 7c.

Example 5: ternary system with three binary compounds

This example illustrates additional issues raised by the presence of a multiple vertex. Let us consider a three-component system of A, B, and E. Two different compounds, C and D, can form between A and B, and another compound,

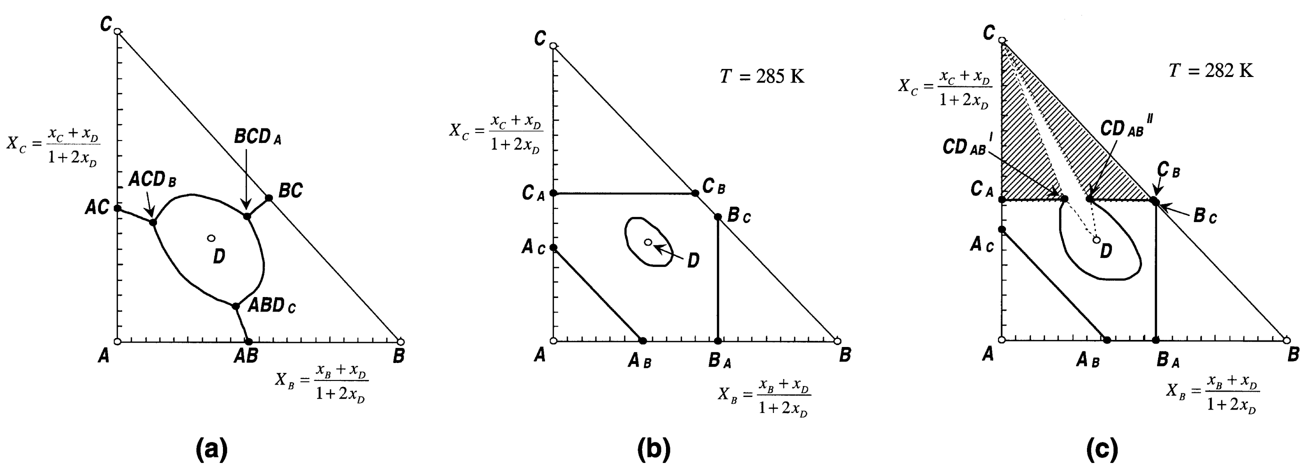

Figure 7. Isobaric phase diagram for system with ternary compound (Example 4).
(a) Polythermal diagram; (b) isothermal cut at 285 K; (c) isothermal cut at 282 K.

F, can form between B and E. The reactions as well as the thermodynamic data are summarized in Table 10.

Figure 8a shows the calculated isobaric phase behavior in a 3-D T-x diagram, and Figure 8b depicts its polythermal projection. The projection is plotted in transformed coordinates, with the horizontal and vertical axes, respectively, corresponding to

$$X_B = \frac{x_B + x_C + 2x_D + 2x_F}{1 + 2x_C + 2x_D + 2x_F} \tag{10a}$$

$$X_E = \frac{x_E + x_F}{1 + 2x_C + 2x_D + 2x_F} \tag{10b}$$

The phase behavior qualitatively resembles the ternary system phenol−o-cresol−2-methyl-2-propanol, studied experimentally by Jadhav et al. (1992). However, due to the ideality assumption, the temperatures of the reactive vertices are generally found to be higher than those observed experimentally.

Three isothermal cuts are depicted in Figure 9. At 295 K, the saturation varieties of A, B, C, D, and E appear as separate regions, each bounded by two vertices and an edge (Figure 9a). The F saturation variety does not appear at this temperature. Note that both C_{ABD} and D_{ABC} are multiple vertices. The constituent vertices are connected to each other by an edge, as Rule 5 suggests. Note that these vertices have to be adjacent to one other vertex ($c - r = 3$ and $n = 1$, thus, $q = 3 - 2 = 1$). At 286 K, the saturation varieties of A, B, C, and D intersect with each other, giving rise to three binary saturation varieties: AC_{BDEF}, CD_{ABEF}, and BD_{ACEF}, respectively (Figure 9b). At 280 K, the C saturation variety intersects with the E saturation variety, causing the appearance of

Table 10. Data for Ternary System with Three Binary Compounds (Example 5)

Pure Component Data		
Component	ΔH_m (J/mol)	T_m (K)
A	11,400	314
B	11,200	298
C	20,200	375
D	17,100	410
E	29,900	304
F	20,450	395
Reaction equilibrium constant: $K = \exp[(E_1 + E_2/T)]$		
Reaction	E_1	E_2 (K)
$2A + B = C$	−17.5	5,500
$A + 2B = D$	−16.2	5,050
$2B + E = F$	−14.1	3,850

a multiple vertex CE_{ABDF} (Figure 9c). Both saturation varieties are divided into two separate regions. The F saturation variety also appears at this temperature. Let us focus on vertex CE_{ABDF}. There are two other vertices commonly saturated with C (AC_{BDEF} and CD_{ABEF}). According to Rule 4, a constituent vertex of CE_{ABDF} can only be adjacent to one other vertex saturated with C. Similarly, there are two other vertices commonly saturated with E (AE_{BCDF} and EF_{ABCD}), while a constituent vertex of CE_{ABDF} can only be adjacent to one of them. The actual correspondence among these vertices is shown in Figure 9c. AC_{BDEF} is not adjacent to CD_{ABEF}, because the edge connecting them is interrupted by the two constituent vertices of CE_{ABDF}. Similarly, AE_{BCDF} is not adjacent to EF_{ABCD} for the same reason. Since each constituent vertex of CE_{ABDF} is already adjacent to two other vertices, there is no edge connecting them (Rule 5).

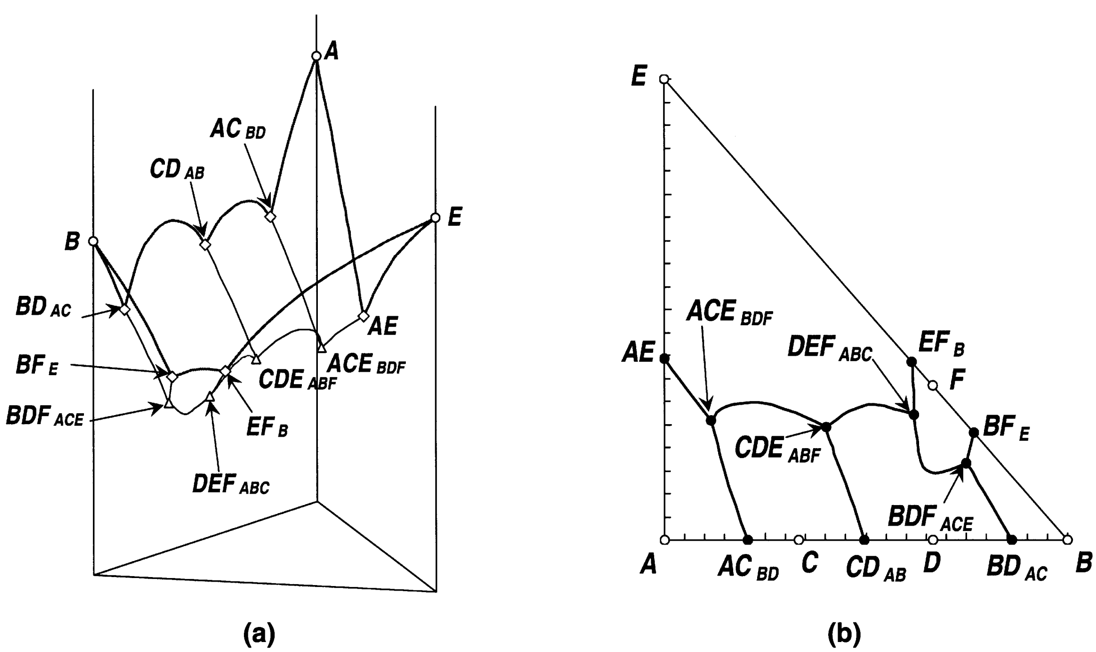

Figure 8. Isobaric phase diagram for ternary system with three compounds (Example 5).
(a) Polythermal diagram; (b) $T - x$ diagram.

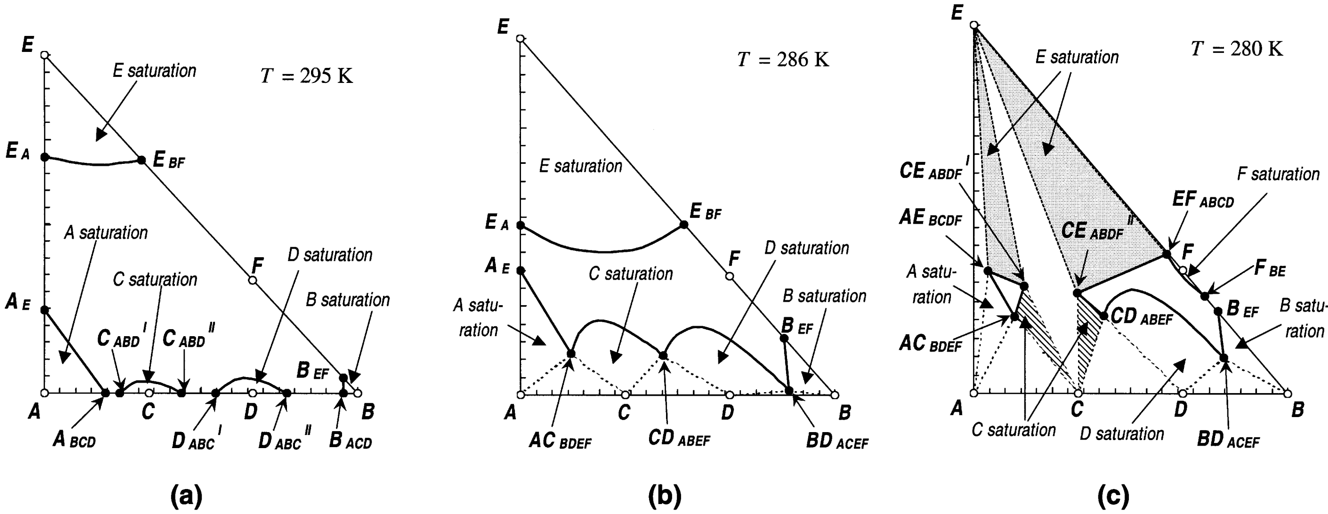

Figure 9. Isobaric isothermal phase diagrams for ternary system with three compounds (Example 5).

(a) At 295 K; (b) at 286 K; (c) at 280 K.

Example 6: four component system with two binary compounds

This example deals with a system consisting of A, B, C, and D, where two binary compounds E and F can form. The input information as well as the reactions involved is given in Table 11. The polythermal phase diagram for this system is shown in Figure 10a. Since $c - r = 4$, three independent transformed coordinates are used in this plot, namely

$$X_B = \frac{x_B}{1 + 3x_E + 2x_F} \tag{11a}$$

$$X_C = \frac{x_C + 3x_E}{1 + 3x_E + 2x_F} \tag{11b}$$

$$X_D = \frac{x_D + x_F}{1 + 3x_E + 2x_F} \tag{11c}$$

The vertices are not labeled to maintain clarity. Figure 10b shows the Jänecke projection of this phase diagram onto the ABC face. To completely represent the phase behavior, two other projections (not shown) are required (Samant et al., 2000).

Three of the faces of the tetrahedron in Figure 10a (ABC, ABD, and ACD) represent ternary system phase behaviors that resemble those of real systems, where A = p-chloronitrobenzene, B = o-chloronitrobenzene, C = p-dichlorobenzene, and D = p-dibromobenzene (Dikshit and Chivate, 1971; Tare and Chivate, 1976). In the absence of a realistic model for predicting activity coefficients, experimental data for ternary systems can be used to fit the parameters of an empirical activity coefficient model. These parameters are then used to better predict the quaternary phase behavior.

Figure 11 shows the isobaric isothermal phase diagram at 296 K. There are 12 vertices and 16 edges bounding 5 single saturation varieties (A, B, C, D, and E) and 6 double saturation varieties (AD, AE, BD, CD, CE, and DE). The F saturation variety does not appear at this temperature. Note that each vertex with one saturated component has two edges ($c - r - 2 = 2$), while each vertex with two or three saturated components has three edges ($c - r - 1 = 3$).

Table 11. Data for Quaternary System with Two Binary Compounds (Example 6)

Pure Component Data		
Component	ΔH_m (J/mol)	T_m (K)
A	16,000	356.7
B	25,000	305.7
C	23,000	326.2
D	28,000	360.7
E	22,000	380
F	29,000	390
Reaction equilibrium constant: $K = \exp[E_1 + (E_2/T)]$		
Reaction	E_1	E_2 (K)
$A + 3C = E$	−14.5	5,000
$2A + D = F$	11.9	−3,500

Conclusions

We have presented a systematic procedure for the generation and visualization of high-dimensional isobaric phase diagrams for systems exhibiting compound formation and/or polymorphism. The key idea is to treat compound formation as reactions, and to consider different polymorphs as distinct in solid form, but the same in liquid form. The reactive phase diagram is basically a reaction-invariant projection of the intersection between reaction equilibrium and solid-liquid phase equilibrium varieties. Congruent and incongruent melting can also be explained as a consequence of reaction and solid-liquid phase equilibrium.

In the literature, phase diagrams with compound formation are plotted by neglecting the composition of the compounds formed (Tavare, 1995). If we have r compounds

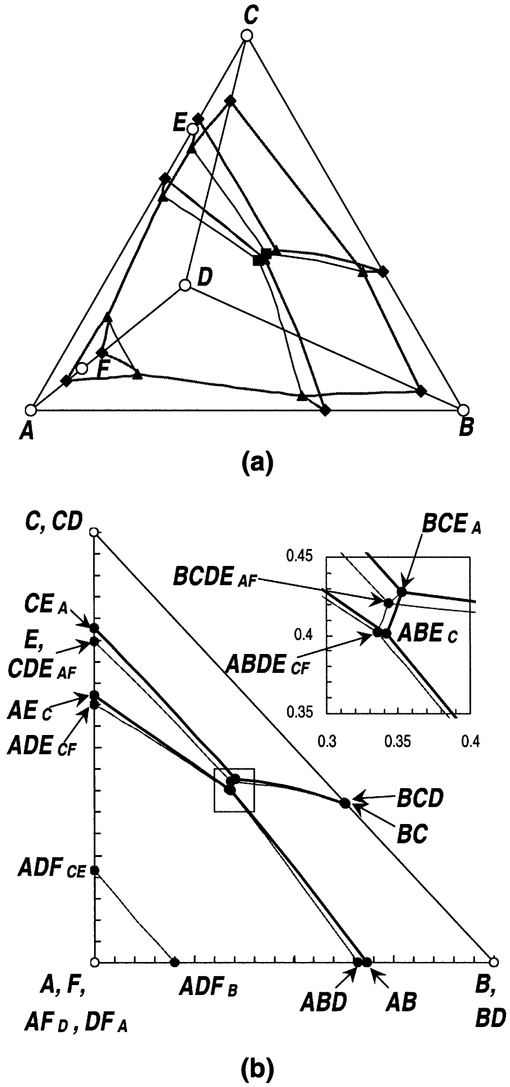

Figure 10. Isobaric phase diagram for quaternary system with two compounds (Example 6).

(a) 3-D polythermal diagram; (b) projection onto ABC plane.

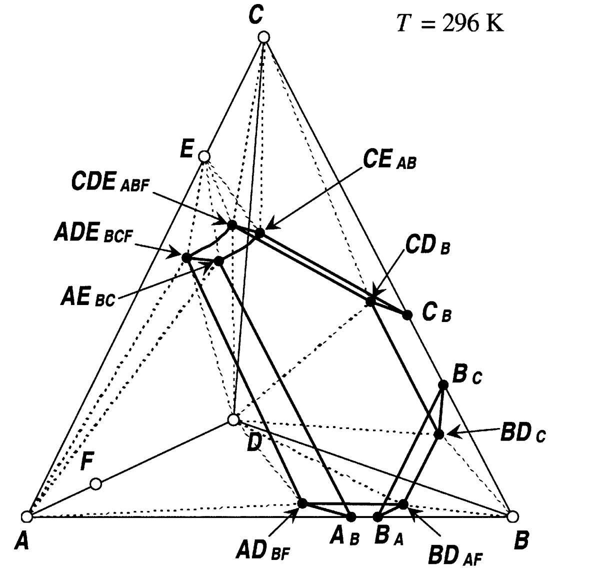

Figure 11. Isobaric isothermal phase diagram at 296 K for quaternary system with two compounds (Example 6).

formed by r compound formation reactions, this is equivalent to plotting the phase diagrams in transformed mole fractions by choosing the r compounds as reference. Thus, in the literature, the phase behavior was plotted in transformed mole fraction space without actually knowing the transforms.

This systematic procedure is expected to play a role in the production of pharmaceuticals, which often involve compounds and polymorphs. The phase diagram showing the size and location of all the saturation varieties in the composition space can be used to help synthesize manufacturing processes for these high-value-added chemicals. Efforts in this direction are under way.

Acknowledgment

Financial support from the National Science Foundation, Grant No. CTS-9908667, is gratefully acknowledged.

Notation

c = number of components
E_1, E_2 = constants
f = number of degrees of freedom
ΔH_m = heat of fusion, $J \cdot mol^{-1}$
i, j, k = indices
k = number of adjacent vertices
K_j = reaction equilibrium constant of reaction j
m = dimension
n = number of saturated components
p = number of unsaturated components
q = total number of edges starting or ending at a vertex
r = number of independent reactions involving non-electrolytes
R = universal gas constant, 8.314 $J \cdot mol^{-1} \cdot K^{-1}$
T = temperature, K
T_m = melting point, K
υ_i, υ_j = vertices
x_i = mole fraction of component i, dimensionless
X_i = transformed coordinate
γ_i = activity coefficient of component i, dimensionless
υ_{ij} = stoichiometric coefficient of component i in reaction j

Superscripts

M = molecular
R = reactive
sat = saturated

Subscripts

P = isobaric
PT = isobaric isothermal

Literature Cited

Beckmann, W., "Seeding the Desired Polymorph: Background, Possibilities, Limitations, and Case Studies," *Org. Proc. Res. Dev.*, **4**, 372 (2000).

Berry, D. A., and K. M. Ng, "Separation of Quaternary Conjugate Salt Systems by Fractional Crystallization," *AIChE J.*, **42**, 2162 (1996).

Berry, D. A., S. R. Dye, and K. M. Ng, "Synthesis of Drowning-Out Crystallization-Based Separations," *AIChE J.*, **43**, 91 (1997).
Berry, D. A., and K. M. Ng, "Synthesis of Reactive Crystallization Processes," *AIChE J.*, **43**, 1737 (1997).
Cisternas, L. A., and D. F. Rudd, "Process Designs for Fractional Crystallization from Solution," *Ind. Eng. Chem. Res.*, **32**, 1993 (1993).
Collet, A., "Separation and Purification of Enantiomers by Crystallization Methods," *Enantiomer*, **4**, 157 (1999).
Dikshit, R. C., and M. R. Chivate, "Selectivity of Solvent for Extractive Crystallization," *Chem. Eng. Sci.*, **26**, 719 (1971).
Dye, S. R., and K. M. Ng, "Bypassing Eutectics with Extractive Crystallization: Design Alternatives and Tradeoffs," *AIChE J.*, **41**, 1456 (1995a).
Dye, S. R., and K. M. Ng, "Fractional Crystallization: Design Alternatives and Tradeoffs," *AIChE J.*, **41**, 2427 (1995b).
Haase, R., and H. Schönert, *Solid-Liquid Equilibrium*, Pergamon, New York (1969).
Iimuro, S., Y. Morimoto, and T. Kitamura, "Process for Preparing High-Purity Bisphenol A," U.S. Patent No. 4,954,661 (1990).
Jadhav, V. K., M. R. Chivate, and N. S. Tavare, "Separation of Phenol from Its Mixture with *o*-Cresol by Adductive Crystallization," *J. Chem. Eng. Data*, **37**, 232 (1992).
Purdon, P. F., and V. W. Slater, *Aqueous Solution and the Phase Diagram*, Arnold, London (1946).
Ricci, J. E., *The Phase Rule and Homogeneous Equilibrium*, Dover Publications Inc., New York (1966).
Samant, K. D., D. A. Berry, and K. M. Ng, "Representation of High-Dimensional, Molecular Solid-Liquid Phase Diagrams," *AIChE J.*, **46**, 2435 (2000).
Schroer, J. W., C. Wibowo, and K. M. Ng, "Synthesis of Chiral Crystallization Processes," *AIChE J.*, **47**, 369 (2001).
Tare, J. P., and M. R. Chivate, "Separation of Close Boiling Isomers by Adductive and Extractive Crystallization," *AIChE Symp. Ser. No. 153*, **72**, 95 (1976).
Tavare, S. N., *Industrial Crystallization: Process Simulation Analysis and Design*, Plenum Press, New York (1995).
Wibowo, C., and K. M. Ng, "Unified Approach for Synthesizing Crystallization-based Separation Processes," *AIChE J.*, **46**, 1400 (2000).
Wibowo, C., and K. M. Ng, "Visualization of High-Dimensional Phase Diagrams of Molecular and Ionic Mixtures," *AIChE J.*, **48**, 991 (May 2002).

Manuscript received Dec. 17, 2001, and revision received Mar. 8, 2002.